Molecular Beam Scattering of Nitrogen Molecules in Supersonic Seeded Beams: A Probe of Rotational Alignment

Vincenzo Aquilanti,*,† Daniela Ascenzi,† David Cappelletti,‡ Roberta Fedeli,† and Fernando Pirani†

Dipartimento di Chimica, Università di Perugia, Via Elce di Sotto 8, 06123 Perugia, Italy, and Istituto per le Tecnologie Chimiche, Università di Perugia, 06125 Perugia, Italy

Received: April 10, 1997; In Final Form: June 10, 1997[⊗]

Measurements of total integral cross sections for scattering of nitrogen molecules by Xe atoms in the glory collision energy range (40−600 meV) are reported under two different experimental conditions, using either a rotationally "hot" (most probable levels $J = 8, 9$) effusive beam of nitrogen (obtaining information on the isotropic component of the interaction potential) or rotationally "cold" N_2 seeded beams emerging from supersonic expansions (obtaining quantitative information on rotational alignment of molecular nitrogen). The scattering results presented in this paper allow us to establish that the recently reported phenomenon of the strong correlation between the degree of collision-induced alignment and the speed of the molecules within a supersonic seeded velocity distribution, as previously observed for the first time in molecular oxygen, also occurs for the case of nitrogen molecules. Alignment parameters are reported for both the *ortho* and *para* forms of nitrogen, which are cooled down in the seeded supersonic expansion process to their lowest rotational levels $J = 0, 1, 2$.

I. Introduction

In previous work reported from our laboratory,[1] we have described in detail how supersonic expansions of gaseous mixtures of molecular oxygen in lighter carriers—seeded molecular beams—not only lead to acceleration of the molecules and to cooling of their internal degrees of freedom but also represent a natural and facile technique for obtaining alignment of molecular rotations.[2] A striking result has been that such an alignment effect, remarkable for all studied carrier gases (in particular for H_2, He, Ne, and their mixtures), depends drastically on the final speed to which molecules are accelerated, so that, for any seeded supersonic expansion, fast molecules are much more highly aligned than slower ones. Such conclusions opened up the way to prepare molecules with well-defined velocities and alignment ratios by adjusting the mixture composition of carrier gases. Our previously cited studies suggested that collisional alignment is a complex phenomenon, which is determined by the high number of collisions among diatomic molecules and carrier gas atoms in the very early region of the expansion, *i.e.*, where the supersonic beam is formed; it should show up every time there is an anisotropic interaction between the molecule and the seeding carrier gas and should be a general phenomenon, particularly for diatomic molecules other than O_2. A similar effect on alignment has been recently observed in mobility measurements for N_2^+ ions in helium.[3]

Subsequently this collisional alignment technique has been used[4] to perform scattering experiments (at thermal energies corresponding to the glory region for total cross sections) between oxygen molecules with a controlled alignment and rare gases (Xe and Kr). In such experiments sizeable differences for both the smooth component of cross sections and the glory interference patterns were observed as the alignment degree was varied. These observations are of interest for two main reasons: first of all, they represent a clear evidence of the fact that total integral cross section data, being sensitive to the molecular alignment, can provide information also on the anisotropic part of the intermolecular potential between projectile molecule and target gas atom; second, they prove that scattering experiments can be exploited as a probe of the molecular alignment when the interaction is known. This probe can be of very general applicability and involves no use of the magnetic analysis technique, which has been employed for the paramagnetic case of O_2[1] but which is clearly inapplicable for most molecules, which are diamagnetic.

Here we report similar scattering experiments with Xe atoms performed with supersonic seeded beams containing another diatomic molecule, nitrogen, which exhibits properties (polarizability and anisotropy, bond length, *etc.*) quite similar to oxygen and for which an alignment effect comparable to the latter can be expected.

In section II we describe the experimental apparatus used for scattering measurements and in section III a detailed description is reported concerning the analysis of total integral cross sections measured by using a rotationally "hot" (most probable levels: $J = 8, 9$) effusive beam of N_2 and Xe as scattering partner. This experiment, which corresponds to a situation where the nitrogen molecule is rotating so fast that an average over orientations is seen by the collision partner, gives information on the spherical (or isotropic) component of the interaction, $V_0(R)$, only dependent on the intermolecular distance R. Section IV is devoted to the description and the analysis of results obtained by using "cold" supersonic seeded beams of nitrogen ($J = 0$, 1, and 2). In particular section IV.A presents data on the average values of total integral cross sections and how to extract information on collision-induced alignment of rotational angular momenta in the beams originated by the seeded expansion; in section IV.B theoretical considerations are developed on how to express the alignment degree for low values of the magnitude of the rotational angular momentum vector, and results for the discrete analogues of multipole moments coefficients are reported for rotational levels $J = 1$ and 2 of N_2. Finally, section IV.C deals with data analysis of the glory pattern shift in total integral cross sections and with

† Dipartimento di Chimica.
‡ Instituto per le Tecnologie Chimiche.
[⊗] Abstract published in *Advance ACS Abstracts,* September 15, 1997.

S1089-5639(97)01237-1 CCC: $14.00

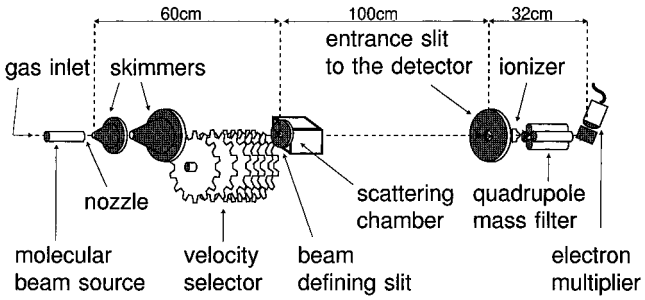

Figure 1. Experimental apparatus: a schematic view.

the extraction of information on the leading term of the anisotropic part of the interaction in N_2-Xe, $V_{anis}(R,\Theta)$, dependent on both R and the angle Θ between the molecular axis and the direction of approach of collision partners. Conclusions will follow in section V.

II. Experimental Section

II.A. The Apparatus. The experimental apparatus (see Figure 1) employed for the measurements described in this paper is the same as used for the O_2 rotational alignment study[1] and scattering experiments with polarized beams.[4] It consists of a set of differentially pumped vacuum chambers where the molecular beam emerging from the source, which can operate under effusive and supersonic conditions, is velocity selected with a resolution of ~5 % (FWHM) by a set of eight rotating slotted disks, before entering into the scattering chamber. The on-line beam intensity after the scattering region is measured by a quadrupole mass spectrometer. The length of the beam path and the dimension of the defining slits provide the stringent angular resolution needed to measure true quantum integral cross sections. The measurements of total (elastic + inelastic) integral cross sections are performed through the attenuation of the velocity selected beam as it crosses the scattering chamber, filled with the target gas (Xe in the present case) in the typical pressure range of $10^{-2}-10^{-3}$ Torr and cooled down to liquid or solid air temperature, to decrease the quenching of the glory interference by the thermal motion of the target gas. Liquid air is introduced in a cryostat attached to the scattering chamber and solid air is produced by a near-adiabatic evaporation of the liquid by pumping at sufficiently high speed. The cryostat temperatures, which have to be kept very stable in time during the measurements, are monitored by a thermocouple and found to correspond to target gas temperatures of ~90 and ~70 K for liquid and solid air cooling, respectively. Under these conditions the selected N_2 beam velocity v practically coincides with the collision velocity of the N_2-Xe system in the center of mass frame.

II.B. Procedure. Two different types of total integral cross section measurements have been carried out:

(*i*) Cross section measurements in the thermal energy range as a function of collision velocity v for the N_2-Xe system using a *rotationally hot* effusive beam of N_2: in these experiments, an effusive beam of nitrogen is produced by expanding pure N_2 (source pressure ~3 Torr) from a nozzle 1.0 mm in diameter; electrical heating wires around the nozzle permit heating of the source (by Joule effect) up to a temperature of 530 ± 5 K. Using this source, a nearly effusive beam can be produced with N_2 molecules in the ground electronic state $^1\Sigma_g^+$ but presenting a hot rotational temperature (300−500 K) and a broad velocity distribution, which allows cross section measurements in a wide velocity range, *i.e.*, from 580 to 2230 m·s^{-1}. Such a procedure permits us to obtain a more stable beam with respect to a previously used microwave discharge source[5] and avoids also the presence of metastable nitrogen molecules, which are produced in small concentration in microwave discharges.

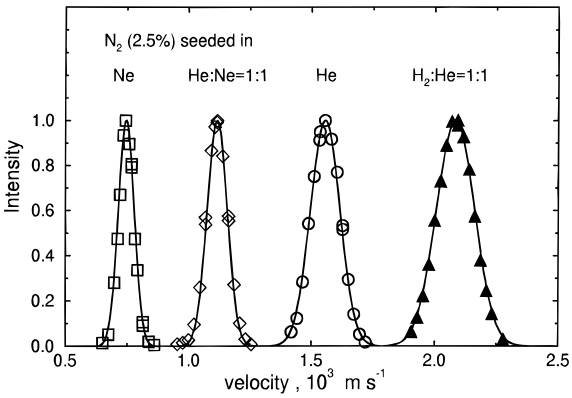

Figure 2. Measured velocity distributions of supersonic beams of N_2 seeded in various carrier gases with variable mixture compositions. Twenty such mixtures have been employed in this work; only four are reported in this figure. Relevant parameters (the peak velocities of the distributions v_{max} and the final translational temperatures T_f), as obtained from a best fit of the measured velocity distributions using formulas appropriate for supersonic seeded beam[26] (full curves), are reported in Table 1.

TABLE 1: Features of the Velocity Distributions of Four Typical Supersonic Molecular Beam Expansions Used in This Experiment and Reported Also in Figure 2

seeding gas[a]	T_f,[b] K	v_{max},[c] km·s^{-1}
H_2:He = 1:1	2.5 ± 0.1	2.08
He	2.0 ± 0.1	1.55
He:Ne = 1:1	2.4 ± 0.1	1.1
Ne	2.5 ± 0.1	0.75

[a] The composition of all the mixtures is 2.5% N_2, and the total source stagnation pressure is 500 Torr for the H_2:He mixture and 800 Torr for all the other seeding gases. The nozzle diameter is ~0.1 mm and the source temperature has been kept constant to ≃290 K. [b] Translational temperature, as obtained from the velocity distributions. [c] Peak velocity.

(*ii*) Cross section measurements for the N_2-Xe system, using rotationally cold nitrogen molecules obtained in the expansion of supersonic seeded beams: the procedure consists of producing supersonic seeded beams of molecular nitrogen using as carrier gases Ne, He, and H_2, either pure or in mixtures whose compositions are varied to cover a wide range of peak velocities v_{max}, from 800 to 2300 m· s^{-1}. An example of velocity distributions obtained using different carriers is reported in Figure 2, where only four different distributions are shown (see also Table 1), but we actually have used about 20 different gas mixtures to adequately cover the whole velocity range. In this case, cross section data are measured as a function of the collision velocity v and for different compositions of the seeding gases, which lead to narrow beam velocity distributions, each one characterized by its peak value v_{max}. A key parameter in these experiments is the ratio v/v_{max} between the selected velocity v and the measured peak velocity v_{max} of each seeded beam.

We recall that[1] magnetic analysis of *paramagnetic* oxygen molecules in seeded supersonic beams has proved a correspondence between the v/v_{max} ratio and the alignment degree; therefore, the use of different mixture compositions of carrier gases, to control the v/v_{max} ratio, has allowed us to measure cross sections as a function of v, at specified values of the alignment degree. Previous collisional experiments with supersonic seeded beams of O_2[4] have shown that total integral cross sections, and their velocity dependence, are sensitive to—and therefore, can be an indirect probe of—molecular

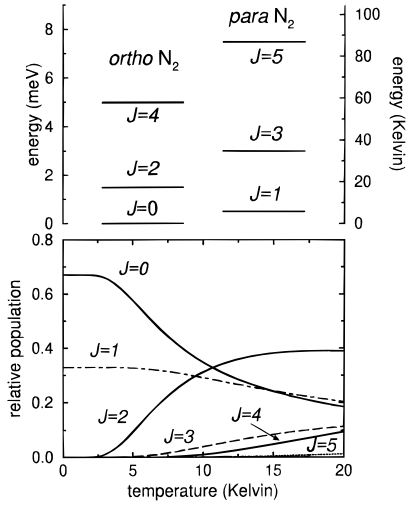

Figure 3. Energy level diagram for the lowest rotational states (J = 0, ..., 5) of $N_2(^1\Sigma_g^+)$ in both the *ortho* and *para* forms (upper panel). In the lower panel, populations are presented for each rotational level as a function of temperature in the range 0−20 K assuming a Maxwell−Boltzmann distribution.

alignment, and this has allowed us to characterize the anisotropic intermolecular potential between O_2 and target atoms, such as Kr and Xe.

Here we apply the same procedure to *diamagnetic* N_2 molecules and measure cross sections, as a function of the collision velocity v at different v/v_{max} ratios, in order to probe the molecular alignment by its effect on scattering cross sections, in a case where magnetic analysis is ineffective. An estimate of the anisotropic interaction at long range between N_2 and Xe will be instrumental to this purpose. In particular we measure cross sections for each mixture at four different velocity ratios v/v_{max} (0.95, 1.0, 1.05, and 1.1) chosen to be the same as for the O_2 system,[4] correlated, in the latter case, to four different alignment degrees.

The supersonic seeded beams used in these experiments show a final translational temperature T_f (see values reported in Table 1) lower than 3 K. Because of collisional relaxation during the expansion, N_2 molecules are expected to have very cold rotational and vibrational temperatures, and in particular the rotational temperature will not be much higher than the final translational temperature T_f. This has also been pointed out in connection with similar experiments on seeded molecular beams of oxygen,[6] and numerous previous studies on supersonic seeded beams of N_2[7] found rotational temperatures T_r in the range 4−9 K, which is quite close to our estimate.

To evaluate the rotational distribution in our supersonic seeded beams, we have to explicitly take into account the nuclear statistics that applies for nitrogen molecules. Since the nuclear spin is 1 for ^{14}N, homonuclear $^{14}N_2$ molecules exist in separate *ortho* (with total nuclear spin I = 0 or 2) and *para* (I = 1) forms;[8] in the ground electronic state ($^1\Sigma_g^+$) two-thirds of the molecules are in the *ortho* form and populate only even (J = 0,2,...) rotational levels, and 1/3 are in the *para* form and populate only odd (J = 1,3,...) rotational levels (see upper panel of Figure 3). The calculated populations of rotational levels for Boltzmann distributions, as a function of rotational temperature in the range 0−20 K, are shown in the lower panel of Figure 3; it can be concluded that under present conditions (rotational temperatures not much higher than 3−4 K) only the rotational levels corresponding to J = 0, 1, 2 are populated. The determination of their relative populations and possible alignment, *i.e.*, nonstatistical distribution of components of the rotational angular momentum **J** along v, will be one of the goals of the following.

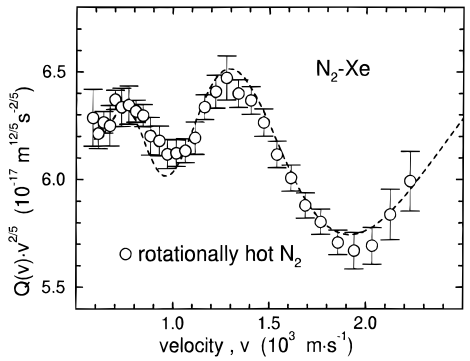

Figure 4. Scattering of a rotationally "hot" effusive nitrogen molecular beam by Xe. Total integral cross sections $Q(v)$ multiplied by $v^{2/5}$ to emphasize the glory pattern (see eq 6) are plotted as a function of collision velocity v. The dashed curve is calculated assuming scattering by a single potential energy curve, corresponding to the isotropic (spherical) interaction $V_0(R)$; see Table 2 and section III.

III. Total Integral Cross Sections from an Effusive Beam and the Spherical Component of the Interaction, V_0 (R)

Total integral cross sections $Q(v)$ for scattering of a rotationally "hot" effusive beam of N_2 (case (*i*) in previous section) by Xe atoms are reported in Figure 4, as a function of collision velocity v in the range 580−2230 m· s^{-1}. As usual they are plotted as $Q(v)v^{2/5}$ to emphasize the glory interference pattern, which provides information on the interaction potential features of the collisional complex. Analogous cross section results have been previously measured by using an effusive nitrogen beam produced from a microwave discharge source;[5] present data are obtained under better experimental conditions (greater stability of the beam and absence of metastable nitrogen molecules, which were instead present in small concentration in the microwave discharge). Assuming Boltzmann distributions of N_2 rotational states, it is found that at 300 K, an estimated lower limit of the rotational temperature of N_2 in the beam, the most populated levels are J = 6 and 7 respectively in *ortho* and *para* forms, whereas at 500 K J = 8 and 9 are correspondingly the most probable levels. Under such conditions the average rotational cycle takes 1.2×10^{-12} s (300 K) and 0.9×10^{-12} s (500 K). These values have to be compared with the typical collisional times, estimated as $8.0 \times 10^{-10}/v$ s (8.0×10^{-10} m represents the average intermolecular distance covered by the projectile during the collision), which vary from 1.4×10^{-12} s to 0.4×10^{-12} s in the collision velocity v range of the present experiment. Taking into account that inelastic transition probabilities are small when high rotational states are involved, that during the collision of a homonuclear diatomic molecule one-quarter of a full rotation is sufficient to average the intermolecular interaction, and that, in effusive beams, N_2 molecules are not only rapidly rotating but also randomly oriented, we can assert that the present scattering data are mainly affected by the spherical average of the full potential energy surface, namely, by the $V_0(R)$ component of the interaction.

As in previous papers[9] we use the MSV (Morse−spline−van der Waals) parameterization to represent this isotropic interaction component, and standard computation techniques are used for elastic cross section calculations in the glory velocity range.[10] The MSV parameterization, expressed by scaling for location R_m and depth ϵ of the potential well:

$$x = \frac{R}{R_m}, \quad f(x) = \frac{V_0(R)}{\epsilon} \tag{1}$$

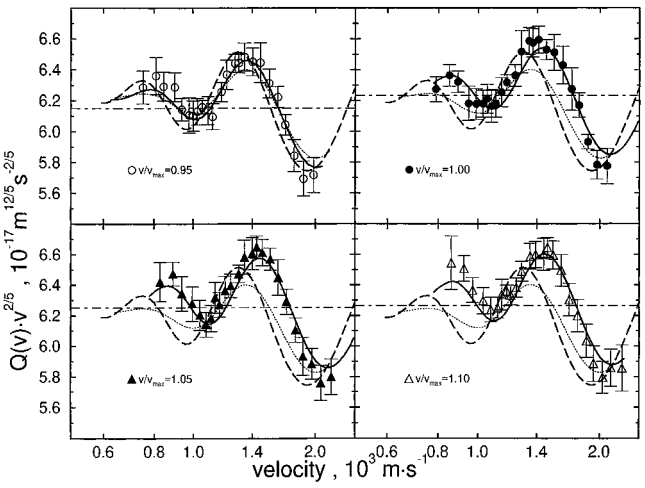

Figure 5. Total integral cross sections, as in Figure 4, for scattering of rotationally "cold" supersonic seeded beams of molecular nitrogen by Xe, at four different values of the v/v_{max} ratios (see section IV). Dashed lines are for scattering by $V_0(R)$, as in the previous figure. Dotted lines are from an IOS calculation; solid lines are calculated according to the "adiabatic" scheme with nonadiabatic coupling as described in section IV.C. In each panel the corresponding $\bar{Q}(v)$s (the "smooth" component, see section IV.A) are reported, multiplied by $v^{2/5}$ (dotted-dashed lines).

is the following:

Morse

$$f(x) = \exp[-2\beta(x-1)] - 2\exp[-\beta(x-1)] \quad \text{for} \quad x \le x_1 \quad (2)$$

spline

$$f(x) = b_1 + (x-x_1)b_2 + (x-x_2)[b_3 + (x-x_1)b_4] \quad \text{for} \quad x_1 < x < x_2 \quad (3)$$

van der Waals

$$f(x) = -\left(\frac{C_6}{\epsilon R_m^6}\right)x^{-6} \quad \text{for} \quad x \ge x_2 \quad (4)$$

The β parameter, which defines the well shape of the potential, is fixed at 6.5 as characteristic of these van der Waals forces;[11] x_1 and x_2 are chosen, as for other previous cases,[9] in the neighborhood of 1.1 and 1.5, while b_1, b_2, b_3, and b_4—the spline parameters—are automatically fixed by imposing that the functions must have the same value and the same derivative at x_1 and x_2. Since the long range constant C_6 are obtained from the absolute value of the measured total integral cross section, with the procedure described in ref 10 and summarized in the next section, only ϵ and R_m are left as parameters to be varied in order to obtain the best agreement between calculated and measured cross sections. The potential parameters for the spherical interaction V_0, so obtained, are reported in Table 2. Values are in very good agreement with previous results:[5] however, because of the higher accuracy achieved by using the present effusive source, the quoted uncertainties on potential parameters (determined from the experimental errors on the glory extrema positions) are considerably lower than before. Total cross sections, first calculated in the center-of-mass reference frame and then convoluted in the laboratory system, are plotted as the dashed line and compared with the experimental results in Figure 4.

TABLE 2: Potential Parameters for N_2−Xe Spherical Interaction $V_0(R)$: MSV Parameterization as Described in the Text and Uncertainties in Parentheses

ϵ, meV	13.70 ± 0.55 (4%)
R_m, Å	4.05 ± 0.08 (2%)
β	6.5
x_1	1.1
x_2	1.55
C_6, meV·m^6	$(1.07 \pm 0.075) \times 10^{-55}$ (7%)

IV. Total Integral Cross Sections from Supersonic Seeded Beams

As noted above (case (*ii*) of section II.B) the N_2 molecules emerging from seeded supersonic expansions are rotationally cooled and only the lowest rotational levels are populated (J = 0, 1, and 2). These levels show a smaller energy separation and a longer rotational cycle than those typical of the previous case. Under such conditions the rotational angular momentum exhibits a strong spatial quantization and could be also preferentially aligned orthogonally to the flight direction. Therefore scattering data measured with such beams are most sensitive to the features of the full potential energy surface and particularly to the anisotropy.

Total integral cross sections for scattering of N_2 as a function of collision velocity v, measured at v/v_{max} = 0.95, 1.00, 1.05, and 1.10, are reported in Figure 5. The observation is made that with increasing v/v_{max} scattering results, when compared with those of the previous section (dashed lines in Figure 5), present both an increase in the average absolute value of the cross sections and a shift in the location of the glory extrema. Both effects are of the same extent as the ones observed in the case of O_2−Xe system.[4] This result can be taken as a manifestation of the alignment of N_2 molecules in supersonic seeded beams which, as previously observed for the O_2 case, increases as a function of v within the same beam. The following analysis, based on the measured increase of the absolute value of the cross sections and on an estimate of the long range behavior of the potential energy surface for the N_2−Xe system from the polarizability anisotropy of N_2 molecule, provides quantitative information on the rotational alignment of N_2 (sections IV.A and IV.B; obtained ranges for the relevant alignment parameters will be wide enough to account for uncertainties in such an estimate). Moreover, the observed shifts in the glory interference pattern depend on both the alignment degree and the anisotropy of the interaction potential at intermediate intermolecular distances. Solid lines in Figure 5 represent cross sections calculated by using the obtained alignment parameters, an assumed interaction anisotropy, and an approximate treatment of the dynamics of N_2−Xe collisions (see section IV.C).

IV.A. Evidence of Rotational Alignment from Its Effect on the Average Scattering Cross Sections. To analyze the effects shown in Figure 5, the collision dynamics is treated following an adiabatic representation in the coupled states framework, developed in our laboratory.[12] This representation considers the centrifugal energy, due to the effect of the impact parameter and decreasing as R^{-2}, as a diagonal term, and the collision is described as evolving along effective adiabatic potentials, obtained by properly taking into account molecular rotations and the electrostatic interaction potential. According to this description, nonadiabatic transitions, which are respon-

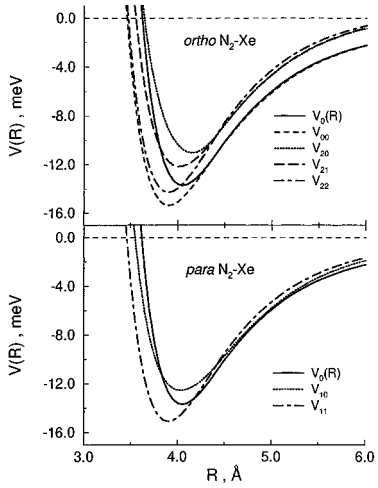

Figure 6. Adiabatic potential energy curves V_{JM} (section IV.C) describing the interaction between N_2 molecule and Xe atom for the *ortho* (upper panel) and *para* (lower panel) forms. The "spherical" component $V_0(R)$ is shown as a solid line.

sible for inelastic events, are localized in restricted R ranges of relevance for the shift of the glory pattern, to be discussed in section IV.C.

Effective potential curves, labeled by the rotational quantum number J and its helicity M (*i.e.*, projection of **J** along the velocity direction v), are obtained by full diagonalization of the secular equation along the lines of[12] assuming a model for the interaction. The curves $V_{JM}(R)$ reported in Figure 6 are actually those corresponding to the final best fit of our analysis.

For the analysis of measured smooth components of cross sections, which are the focus here for their important information content on the alignment in the beam, an accurate close formula for V_{JM} can be derived from a perturbation expansion around the librating rotor limit.[12]

Following a semiclassical view of molecular scattering from a single potential energy curve in the glory energy range, the elastic integral cross section $Q(v)$ as a function of the relative collision velocity v can be written as[10]

$$Q(v) \simeq \bar{Q}(v) + Q_{glory}(v) \tag{5}$$

where $Q_{glory}(v)$ is an oscillatory term and $\bar{Q}(v)$ is the smooth (average) component of the cross section to which phase shifts associated with large impact parameters mainly contribute. The latter essentially depends on the long range part of the interaction, and in the case of a purely attractive potential $-C_s/R^s$ it can be expressed as[13]

$$\bar{Q}(v) = g(s)\left(\frac{2\pi C_s}{hv}\right)^{2/(s-1)} \tag{6}$$

where h is the Planck constant and the $g(s)$ coefficient is given in terms of Γ functions. Accordingly the measurement of the absolute value of the average cross section $\bar{Q}(v)$ provides information on the long range attraction.

The $\bar{Q}$ term mainly probes the attractive potential in the neighborhood of the intermolecular distance corresponding to the "limiting" impact parameter given by$(\bar{Q}/2\pi)^{1/2}$ [14] (6.5−8 Å in our case). In this distance range the first term of a multipole expansion in neutral−neutral systems, namely, the $-C_6/R^6$ dipole−dipole term, gives the main contribution to $\bar{Q}$. Therefore the working formula

$$\bar{Q}(v) = (6.039 \times 10^5)\left(\frac{C_6}{v}\right)^{2/5} \tag{7}$$

provides direct information on the C_6 potential parameter ($\bar{Q}$ is given in m^2 if C_6 is expressed in meV·m^6 and the velocity v in $m \cdot s^{-1}$).

The C_6 so obtained must be taken as an effective dipole−dipole interaction constant, since it includes smaller contributions from higher order terms of the multipole expansion.

In the case of an anisotropic potential, $\bar{Q}(v)$ can be defined, in the adiabatic picture, as a weighted sum of contributions coming from each of the adiabatic potential energy curves V_{JM} (Figure 6), the weighting factors being related to the molecular alignment. Therefore the increase of the measured $\bar{Q}(v)$ values, as a function of v/v_{max}, depends not only on the strength and anisotropy of the long range attraction but also on the variation of the molecular alignment degree.

Treatment of the dynamics as evolution along adiabatic potential energy curves is accurate for $\bar{Q}(v)$, since at long range no couplings persist among rotational states. In addition also the helicity mixing, due to Coriolis forces, can be neglected here but will be of interest in the following analysis of the glory interference pattern.

The long range anisotropy in the potential can be expressed as[15]

$$-\frac{C_6^{anis}}{R^6} \simeq -\frac{C_6}{R^6}\left(\frac{\alpha_{||} - \alpha_{\perp}}{3\bar{\alpha}}\right) \tag{8}$$

where the C_6/R^6 term, as seen before, defines the long range attraction of the isotropic potential V_0; $\alpha_{||}$ and $\alpha_{\perp}$ are the parallel and perpendicular polarizabilities of N_2, respectively, which also enter the definition of the mean value of the polarizability $\bar{\alpha} = (\alpha_{||} + 2\alpha_{\perp})/3$. For this system C_6 has been determined as discussed in section III by scattering experiments with the rotationally "hot" effusive beam and its value is reported in Table 2. For the polarizability anisotropy $(\alpha_{||} - \alpha_{\perp})/3\bar{\alpha}$, values in the literature range from 0.14−0.15 (recent experimental[16] and theoretical[17] results) to 0.19.[18] We have chosen an intermediate value of 0.17, which is higher than the most recent results. Actually scattering cross sections $\bar{Q}(v)$ probe intermolecular interactions in a distance range (here 6.5−8 Å) where the attraction essentially depends on the dipole−dipole interaction but the effect of higher order terms is not negligible. The relative anisotropy of refs 16 and 17 describes only the effect of anisotropic dipole−dipole attraction: this leads to an underestimate of the contributions coming from higher order terms, as clearly pointed out by Thuis *et al.*[19] for the case of NO−Xe interaction.

As discussed in section II.B only the rotational levels $J = 0$, 1, 2 are significantly populated at the rotational temperature typical of the seeded supersonic beams of N_2 used in the present scattering experiments. Accounting for the allowed helicity states implies that only six adiabatic potential energy curves (see Figure 6) are relevant for the analysis of the present results. Deviations in the long range behavior of the adiabatic curves V_{JM} from that of the isotropic component V_0 are expected to be responsible for the variation of the measured absolute value of the $\bar{Q}(v)$ component of cross sections, when the population of JM sublevels is varied. This situation must be contrasted with that of the experiments described in the previous section, where molecules were randomly oriented and rotating fast enough to average their anisotropy, leading to an effective interaction corresponding to the spherical potential V_0.

The asymptotic behavior of the V_{JM} curves can be accurately given by perturbation theory of the rigid rotor, as described in the formulas reported in the appendix of ref 12, here corrected for a misprint:

$$V_{JM}(R) = BJ(J+1) - \frac{C_6}{R^6} + \frac{J(J+1) - 3M^2}{(2J+3)(2J-1)}\left(-\frac{C_6^{anis}}{R^6}\right) \quad (9)$$

$$+ \frac{9}{8(2J+1)}\left[\frac{(J^2-M^2)(J-M-1)(J+-1)}{(2J-1)^3(2J-3)} - \frac{(J-M+2)(J-M+1)(J+M+2)(J+M+1)}{(2J+3)^3(2J+5)}\right]\left(-\frac{C_6^{anis}}{R^6}\right)^2\frac{1}{B}$$

$$+ \textit{3rd order term}$$

where $B = 0.2491$ meV is the rotational constant of the nitrogen molecule.[8] Curves reported in Figure 7 are calculated by using the value of C_6 and C_6^{anis} obtained as described above.

In the R range which mainly influences the magnitude of the cross sections, first and second order terms in eq 9 dominate and the ratios between the smooth components for scattering by each of the adiabatic potential curves, V_{JM}, and that for scattering by the isotropic component, V_0, can be calculated as

$$\frac{\bar{Q}_{JM}}{\bar{Q}_0} = \left(\frac{V_{JM} - BJ(J+1)}{V_0}\right)^{2/5} \quad (10)$$

which in turn gives the fractional deviations defined as

$$\Delta\bar{Q}_{JM} = \left(\frac{\bar{Q}_{JM}}{\bar{Q}_0} - 1\right) \quad (11)$$

The experimentally measured quantities $\bar{Q}$, shown as dotted-dashed lines in Figure 5, are properly weighted averages of $\bar{Q}_{JM}$. The weights w_{JM}, their determination and particularly whose deviations from statistical, are the target of the present analysis, which exploits the following relationship:

$$\Delta\bar{Q} = \frac{\bar{Q} - \bar{Q}_0}{\bar{Q}_0}\sum_{JM} w_{JM}\Delta\bar{Q}_{JM} \quad (12)$$

The quantity $\Delta\bar{Q}$ represents the shift of the smooth component of cross sections, which we have measured (Figure 5) at four values of the v/v_{max} ratio and can be obtained by inserting the results of eqs 9−11 in eq 12.:

$$\Delta\bar{Q}\ 2.73w_{10} - 1.33w_{11} + 0.14w_{00} + 1.82w_{20} + 1.00w_{21} - 1.95w_{22} \quad (13)$$

The weights w_{JM}, which must add to one, must also satisfy the nuclear statistics appropriate for nitrogen molecules. In the present case they must satisfy the conditions

$$w_{00} + w_{20} + w_{21} + w_{22} = {}^2/_3 \quad \text{for the } \textit{ortho} \text{ form } (J = 0 \text{ and } 2)$$

$$w_{10} + w_{11} = {}^1/_3 \quad \text{for the } \textit{para} \text{ form } (J = 1)$$

Under statistical conditions (no alignment, see Table 3), $\Delta\bar{Q}$ can be checked to be zero. The previous formulas allow us to establish ranges of variation of the weights from their statistical values when $\Delta\bar{Q}$ is different from zero. Table 3 lists such ranges for the case $v/v_{max} = 1.10$. It has to be noted that the largest increase in the relative weights is observed for the sublevels 20 and 10, corresponding to molecules rotating in a plane parallel to the flight direction. The small upper limit for w_{00} indicates that relaxation to the ground state $J = 0$, which corresponds to no alignment, is ineffective. The four v/v_{max} ratios considered in our experiments show, as in the case of O_2,[1] that alignment is negligible at the lowest value, 0.95, where accordingly we measure $\Delta\bar{Q} \simeq 0$. The case $v/v_{max} = 1.10$ presents the largest $\Delta\bar{Q}$ and therefore corresponds to the largest alignment effect. This trend is in agreement with the increase in alignment as v/v_{max} increases, first observed in seeded supersonic expansions of O_2.[1]

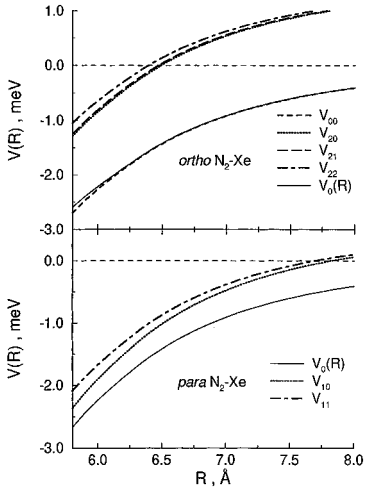

Figure 7. Long range behavior of the adiabatic potential energy curves of Figure 6 (see also section IV.A).

TABLE 3: Relative Population w_{JM} of JM Sublevels Corresponding to Nitrogen Molecules Traveling at $v/v_{max} = 1.10$

JM	w_{JM}[a]	w_{JM}[b]
1 0	$0.26 \div {}^1/_3$	0.11
1 1	$0.00 \div 0.07$	0.22
0 0	$0.00 \div 0.18$	0.63
2 0	$0.31 \div {}^2/_3$	0.008
2 1	$0.00 \div 0.36$	0.016
2 2	$0.00 \div 0.08$	0.016

[a] Relative weights as determined by our analysis. [b] Statistical weights corresponding to a rotational temperature $T_r = 4$ K.

IV.B. Quantum-Mechanical Parameterization of Rotational Alignment. The present results on N_2 provide data on molecular alignment which will now be used to obtain alignment parameters for the rotational angular momenta corresponding to $J = 1$ and 2. For such low J states, which correspond to extreme quantum conditions, it is not appropriate to represent the anisotropy in the M distribution by the moments of a classical Legendre polynomial expansion: such an expansion, used in previous work,[2] applies under "semiclassical" conditions, *i.e.*. in the high J limit, since it assumes a continuous distribution of angular momenta.

A representation for alignment parameters for low J values will now be given, closely related to the usual spherical tensor description of orientation;[20,21] to establish the proper normalization for the correspondence of the quantum formulation to the classical high J limit, our simple derivation makes recourse to a discretization of the classical expression for the spatial distribution of the rotational angular momentum vector **J**:

$$n_J(\theta) = N_J \sum_{l=0...}^{\infty} a_l P_l(\cos\theta) \quad (14)$$

Here N_J is the total number of molecules in the rotational level J, $n_J(\theta)$ is the number of molecules whose **J** vector forms an

angle θ with respect to the molecular beam direction and a_l are the classical *multipole moments*:

$$a_l = \frac{(l+1/2)}{N_J}\int_0^{\pi} n_J(\theta) P_l(\cos\theta)\sin\theta\, d\theta, \quad l = 0,2,4,\ldots \tag{15}$$

Following the lines presented in a previous work on the potential expansion in discrete harmonics,[22] we use the relationship that ties Legendre polynomials and particular vector coupling coefficients with large angular momenta:

$$P_l(\cos\theta) = \lim_{J\to\infty}\left[\frac{(2J+1)}{(2l+1)}\right]^{1/2}(-)^{J-M-l}\langle JJM - M|l0\rangle \tag{16}$$

in which the identification holds:

$$\cos\theta = -2M/(2J+1) \tag{17}$$

where the integer M varies from $-J$ to J, discretizing the θ range (from 0 to π) by a grid of $2J+1$ points. Equation 16 allows us to write the discrete analogue of eq 15 and to obtain the quantum expression for the relative population of sublevel n_J^M:

$$n_J^M = N_J(2J+1)^{1/2}\sum_{l=0,\ldots}^{2J}(-)^{J-M-l}\frac{1}{(2l+1)^{1/2}}\langle JJM - M|l0\rangle a_l^J \tag{18}$$

in terms of the discrete analogues of the classical multipole moments of the angular momentum distribution a_l^J. The latter are explicitly given by inverting eq 18 using the orthogonal properties of vector coupling coefficients:

$$a_l^J = \frac{1}{N_J}\left(\frac{2l+1}{2J+1}\right)^{1/2}\sum_{M=-J,\ldots}^{+J}(-)^{J-M-l}\langle JJM - M|l0\rangle n_J^M \tag{19}$$

Explicit expressions for $J = 1$ are

$$a_0^1 = \frac{1}{3N_1}(n_1^0 + 2n_1^1)$$

$$a_2^1 = \frac{(10)^{1/2}}{3N_1}(n_1^1 - n_1^0) \tag{20}$$

and

$$n_1^0 = N_1\left[a_0^1 - \left(\frac{2}{5}\right)^{1/2} a_2^1\right]$$

$$n_1^1 = N_1\left[a_0^1 + \left(a_0^1 + \frac{1}{10}\right)^{1/2} a_2^1\right] \tag{21}$$

while for $J = 2$:

$$a_0^2 = \frac{1}{5N_2}(2n_2^2 + 2n_2^1 + n_2^0)$$

$$a_2^2 = \frac{1}{N_2}\left(\frac{2}{7}\right)^{1/2}(2n_2^2 - n_2^1 - n_2^0)$$

$$a_4^2 = \frac{3}{5N_2}\left(\frac{2}{7}\right)^{1/2}(n_2^2 - 4n_2^1 + 3n_2^0) \tag{22}$$

and

$$n_2^0 = N_2\left[a_0^2 - \left(\frac{2}{7}\right)^{1/2} a_2^2 + \left(\frac{2}{7}\right)^{1/2} a_4^2\right]$$

$$n_2^1 = N_2\left[a_0^2 - \frac{1}{2}\left(\frac{2}{7}\right)^{1/2} a_2^2 - \frac{2}{3}\left(\frac{2}{7}\right)^{1/2} a_4^2\right]$$

$$n_2^2 = N_2\left[a_0^2 + \left(\frac{2}{7}\right)^{1/2} a_2^2 + \frac{1}{6}\left(\frac{2}{7}\right)^{1/2} a_4^2\right] \tag{23}$$

For the present application, where only alignment is involved, the previously determined weights w_{JM} correspond to both positive and negative values of the projection M, and therefore $w_{JM} = 2\, n_J^M$. These formulas allow us to obtain the corresponding a_l^J and a plot of the $-a_2^J/a_0^J$ ratio is presented in Figure 8. In the same figure, the previously obtained alignment data[1] for supersonic seeded O_2 beams are also shown for comparison. An extreme quantum mechanical alignment (corresponding to a classical rotor flying "edge-on" along the beam direction) is described in the above formulas assuming that only $M = 0$ states are populated. In this limit, the ratios $-a_2^J/a_0^J$ are $10^{1/2}$ for $J = 1$ and $5(2/7)^{1/2}$ for $J = 2$: they are also shown in Figure 8.

For $J = 2$, a_4^2 parameters are also of interest, but their determination involves high uncertainties. Estimated ratios a_4^2/a_0^2 range from 1.5 ± 1.5 for $v/v_{max} = 0.95$ (tail of the beam) to 3.0 ± 2.0 for $v/v_{max} = 1.10$ (head of the beam). For reference, note that an unaligned beam for $J = 2$ implies $a_4^2/a_0^2 = 0$, while the "edge-on" configuration corresponds to $a_4^2/a_0^2 = 9(2/7)^{1/2}$.

The relationship of the presently introduced parameters a_l^J to the $A_q^{(l)}(J)$ of the usual description of orientation and alignment, which uses the formalism of spherical tensors[23] and density matrices, can be established for low J values by a comparison between the above formulas and those in refs 20 and 21 (see Table 4).

Values and trends of alignment shown in Figure 8 demonstrate that the overall features of the phenomenon are very much in line with previous observations on molecular oxygen.[1] It should be noted that the observed alignment effect under the present experimental conditions may be only a lower limit of the one that could be measured as the beam is emerging out of the supersonic expansion. A natural depolarization effect in the rotational alignment may arise from coupling of **J** with nuclear spin **I** to give **F**. For the low lying rotational states of nitrogen in its ground vibrational state, of interest here, the hyperfine interaction is very small and the estimated precession time of **J** and **I** around **F** is of the order of $\simeq 10^{-4}$ s,[24] which is comparable with the flight time from the source to the scattering chamber, possibly producing some depolarization effect. On the other hand, the time which typically elapses between two successive collisions is of the order of 10^{-8} s. This is too short to destroy the alignment in the supersonic expansion process, where the interaction which is active during collisions keeps **J** and **I** decoupled.

IV.C. Analysis of Glory Pattern Shift. The quantitative information on the N_2 alignment from previous sections allows us to analyze the glory pattern shift, observed as the parameter v/v_{max} increases. The glory pattern and its shift are sensitive to both the interaction anisotropy in the region around the minima of the potential energy surface and the alignment degree.

The electrostatic interaction potential between the N_2 molecule and the Xe atom is as usual represented by a Legendre polynomial expansion

$$V(R,\Theta) \simeq V_0(R) + V_2(R)P_2(\cos\Theta)\ldots \tag{24}$$

where for the present discussion higher order terms are neglected.

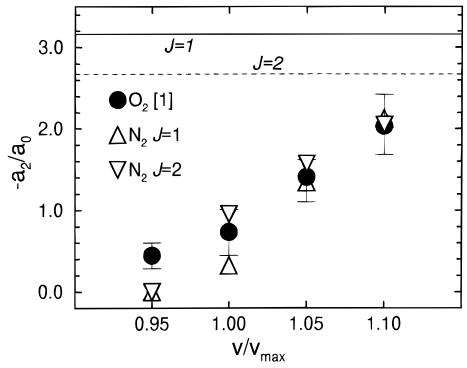

Figure 8. Alignment parameters (section IV. B) $-a_2^J/a_0^J$ as a function of the velocity ratios v/v_{max} for rotational levels $J = 1$ and 2 of N_2, as obtained from present work. Plotted values describe a lower limit for the alignment degree as obtained by taking the w_{JM} within their ranges of variation (see section IV. A). Also shown are data for O_2, obtained from previously reported polarization data.[1] Lines labeled as $J = 1$ and $J = 2$ correspond to the limiting values of the $-a_2/a_0$ parameter ratio where only $M = 0$ components are populated (exclusive alignment in the "edge-on" configuration). The high J (classical) limit is $-a_2/a_0 = 2.5$.

TABLE 4: Correspondence between Discrete Multipole Moments a_l^J [a] and Alignment Parameters $A_0^{(l)}(J)$ [b]

$J = 1$	$a_0^1 = {}^1/_3 A_0^{(0)}(1)$
	$a_2^1 = (10^{1/2}/3) A_0^{(2)}(1)$
$J = 2$	$a_0^2 = {}^1/_5 A_0^{(0)}(2)$
	$a_2^2 = ({}^2/_7)^{1/2} A_0^{(2)}(2)$
	$a_4^2 = {}^{36}/_5\,({}^2/_7)^{1/2} A_0^{(4)}(2)$

[a] Present work, eqs 19, 20, and 22. [b] Reference 21, eq 26, and references therein.

In analogy with the O_2-Xe case,[4] we take

$$V_2(R) = A \exp(-\alpha R) - C_6^{anis} R^{-6} \qquad (25)$$

where A and α have to be determined via a best fitting of the glory scattering pattern at different v/v_{max}, while the anisotropy of the attractive part is the one discussed in section IV.A (cf. eq 8).

Initially a fit of experimental cross section data with an IOS (infinite order sudden) dynamical calculation was attempted; some results are reported in Figure 5 as dotted lines. It can be seen that a reasonable agreement with cross section data at $v/v_{max} = 0.95$ can be obtained, but this calculation completely fails to reproduce the scattering data at the other v/v_{max}.

Following the lines of our previous work involving O_2[4] a more accurate description implies the formulation of an "adiabatic" scheme, implemented by taking into account those nonadiabatic transitions which are important between the rotational levels 0 and 2 for the *ortho* form and 1 and 3 for the *para* form. In particular we have assumed a statistical population of rotational levels (see Table 2) in the case of scattering data at $v/v_{max} = 0.95$; for experiments at other v/v_{max} values, we have taken the mean values in the ranges of relative populations obtained from the previous analysis.

Similarly to the oxygen case,[4] for the *para* form, Coriolis coupling is assumed to completely mix $M = 0$ and 1 helicity states for $J = 1$ and nonadiabatic coupling between $J = 1$ and 3 is included. For the *ortho* form only Coriolis coupling mixing was considered for the $J = 2$ channel, nonadiabatic coupling to the distant level $J = 4$ being neglected.

Cross section calculations performed according to this approach are reported in Figure 5 as solid lines. The obtained parameters for the anisotropic component of the interaction are $A = 7.0 \times 10^6$ meV and $\alpha = 3.37$ Å^{-1}.

V. Summary and Final Remarks

The isotropic component of the interaction for the N_2-Xe system has been obtained from scattering experiments with a rotationally "hot" effusive nitrogen beam. Scattering experiments using supersonic seeded beams of rotationally "cold" nitrogen have proved to be an effective probe for the quantitative determination of the degree of collision-induced alignment of rotational angular momentum in N_2. The alignment parameters which have been derived for the description of the anisotropy in rotational angular momentum distributions under the quantum conditions (low J values) of interest here indicate that both extent and final speed dependence are similar for N_2 and for the previously investigated O_2 case.[1] Therefore we are inclined to suggest (see also ref 3) that the observed alignment effect is a quite general phenomenon. An estimate of the interaction anisotropy in the N_2-Xe system has been obtained from a fit of the glory interference pattern and from its shift as a function of rotational alignment of molecular nitrogen. The simplifications in the dynamical treatment, which involves an adiabatic scheme but with an estimate of nonadiabaticities—which were shown to be reliable for the O_2-Xe system[4]—may have a more limited validity for the N_2-Xe case, where a higher number of effective adiabatic curves is involved and a more accurate treatment of inelastic and nonadiabatic events may be necessary. Further and more detailed information on anisotropy in the well region could be obtained once close coupling calculations for total integral cross section (which are in progress, using the MOLSCAT package[25]) become available.

Acknowledgment. This work is supported by the Italian National Research Council (CNR), by the Ministero dell'Università e della Ricerca Scientifica e Tecnologica (MURST), by the European Union through the programmes Training and Mobility of Researchers Network "Potential Energy Surfaces for Molecular Spectroscopy and Dynamics" (Contract ERB-FMRX-CT96-0088), and by the COST D-3 action.

References and Notes

(1) Aquilanti, V.; Ascenzi, D.; Cappelletti, D.; Pirani, F. *Nature* **1994**, *371*, 399. Aquilanti, V.; Ascenzi, D.; Cappelletti, D.; Pirani, F. *J. Phys. Chem.* **1995**, *99*, 13620.

(2) For relevant work on collisional alignment, see: Sinha, M. P.; Caldwell, C. D.; Zare, R. N. *J. Chem. Phys.* **1975**, *61*, 491. Pullmann, D. P.; Herschbach, D. R. *J. Chem. Phys.* **1989**, *90*, 3881. Pullman, D. P.; Friedrich, B.; Herschbach, D. R. *J. Chem. Phys.* **1990**, *93*, 3224; *J. Phys. Chem.* **1991**, *95*, 8118. Saleh, H. J.; McCaffery, A. J. *J. Chem. Soc., Faraday Trans.* **1993**, *89*, 3217. Weida, M. J.; Nesbitt, D. J. *J. Chem. Phys.* **1994**, *100*, 6372.

(3) Anthony, E. B.; Schade, W.; Bastian, M. J.; Bierbaum, V. M.; Leone, S. R. *J. Chem. Phys.* **1997**, *106*, 5413.

(4) Aquilanti, V.; Ascenzi, D.; Cappelletti, D.; Franceschini, S.; Pirani, F. *Phys. Rev. Lett.* **1995**, *74*, 2929.

(5) Cappelletti, D.; Liuti, G.; Luzzatti, E.; and Pirani, F. *J. Chem. Phys.* **1994**, *101*, 1225.

(6) Amirav, A.; Even, U.; Jortner, J.; Kleinman, L. *J. Chem. Phys.* **1980**, *73*, 4217. Mettes, J.; Heijmen, B.; Reuss, J.; Lainè, D. C. *Chem. Phys.* **1984**, *87*, 1. Matsumoto, T.; Kuwata, K. *Chem. Phys. Lett.* **1990**, *171*, 314.

(7) Miller, D. R.; Andres, R. P. *J. Chem. Phys.* **1967**, *46*, 3418. Luijks, G.; Stolte, S.; Reuss, J. *J. Chem. Phys.* **1981**, *62*, 217. Faubel, M.; Weiner, E. R. *J. Chem. Phys.* **1981**, *75*, 641. Hernandez, S. P.; Dagdigian, P. J.; Doering, J. P. *Chem. Phys. Lett.* **1982**, *91*, 409. Neitzke, H. P.; Terlutter, R. *J. Phys. B* **1992**, *25*, 1931.

(8) Herzberg, G. *Molecular Spectra and Molecular Structure*; Van Nostrand Company Inc.: Princeton−New York, 1967; Vol. I, pp 133−140.

(9) Aquilanti, V.; Candori, R.; Cappelletti, D.; Luzzatti, E.; Pirani, F. *Chem. Phys.* **1990**, *145*, 293. Aquilanti, V.; Cappelletti, D.; Lorent, V.; Luzzatti, E.; Pirani, F. *Chem. Phys. Lett.* **1992**, *192*, 153. Aquilanti, V.; Cappelletti, D.; Lorent, V.; Luzzatti, E.; Pirani, F. *J. Phys. Chem.* **1993**,

97, 2063. Aquilanti, V.; Cappelletti, D.; Pirani, F. *J. Chem. Soc., Faraday Trans.* **1993**, *89*, 1467.

(10) Pirani, F.; Vecchiocattivi, F. *Mol. Phys.* **1982**, *45*, 1003.

(11) Aquilanti, V.; Cappelletti, D.; Pirani, F. *Chem. Phys.* **1996**, *209*, 299.

(12) Aquilanti, V.; Beneventi, L.; Grossi, G.; Vecchiocattivi, F. *J. Chem. Phys.* **1988**, *89*, 751.

(13) Bernstein, R. B.; Kramer, K. H. *J. Chem. Phys.* **1963**, *38*, 2507.

(14) Ury, G. B.; Wharton, L. *J. Chem. Phys.* **1972**, *56*, 5832.

(15) Buckingham, A. D. *Adv. Chem. Phys.* **1967**, *12*, 107.

(16) Experimental values for the polarizability anisotropy of $N_2(^1\Sigma_g^+)$: Bridge, N. J.; Buckingham, *A. D. Proc. R. Soc. London Ser. A* **1966**, *295*, 334. Alms, G. R.; Burnham, A. K.; Flygare, W. H. *J. Chem. Phys.* **1975**, *63*, 3321.

(17) Theoretical values for the polarizability anisotropy of $N_2(^1\Sigma_g^+)$: Spelsberg, D.; Meyer, W. *J. Chem. Phys.* **1994**, *101*, 1282. Bishop, D. M.; Cybulski, S. M. *J. Chem. Phys.* **1994**, *101*, 2180.

(18) Hirschfelder, J. O.; Curtiss, C. F.; Bird, R. B. *The Molecular Theory of Gases and Liquids*; Wiley: New York, 1954. Denbigh, K. G. *Trans. Faraday Soc.* **1940**, *36*, 436.

(19) Thuis, H.; Stolte, S.; Reuss, *J. Chem. Phys.* **1979**, *43*, 351. Thuis, H. H. W.; Stolte, S.; Reuss, J.; van den Biesen, J. J. H; van den Meijdenberg, C. J. N. *Chem. Phys.* **1980**, *52*, 211.

(20) Greene, C. H.; Zare, R. N. *Annu. Rev. Phys. Chem.* **1982**, *33*, 119. Zare, R. N. *Angular Momentum-Understanding spatial aspects in chemistry and physics*; Wiley: New York, 1988; pp 226−242.

(21) Orr-Ewing, A. J.; Zare, R. N. *Annu. Rev. Phys. Chem.* **1994**, *45*, 315.

(22) Aquilanti, V.; Grossi, G. *Lett. Nuovo Cimento* **1985**, *42*, 157. Aquilanti, V.; Cavalli, S.; Grossi, G. *Theor. Chim. Acta* **1991**, *79*, 283. See also: Aquilanti, V.; Cavalli, S.; Grossi, G.; Anderson, R. W. *J. Phys. Chem.* **1993**, *97*, 2443. Note that in this application vector coupling coefficients play the role of discrete polynomials of the Hahn family (Aquilanti, V.; Cavalli, S.; De Fazio, D. *J. Phys. Chem.* **1995**, *99*, 15694).

(23) Fano, U. *Rev. Mod. Phys.* **1957**, 29, 74. Fano, U.; Macek, J. H. *Rev. Mod. Phys.* **1973**, *45*, 553.

(24) De Santis, D.; Lurio, A.; Miller, T. A.; Freund, R. S. *J. Chem. Phys.* **1973**, *58*, 4625. Chan, S. I.; Baker, M. R.; Ramsey, N. F. *Phys. Rev.* **1964**, *136*, A1224.

(25) Hutson, J. M.; Green, S. MOLSCAT computer code, distributed by Collaborative Computational Project No. 6 of the Engineering and Physical Sciences Research Council (U.K.).

(26) Miller, D. R. In *Atomic and Molecular Beam Methods*; Scoles, G., Ed.; Oxford University Press: New York, 1988; Vol. 1, Chapter 2. Anderson, J. B.; Andres, R. P.; Fenn, J. B. *Adv. Chem. Phys.* **1966**, *10*, 275.